3624 *Macromolecules* **2010**, *43*, 3624–3633
DOI: 10.1021/ma9025256

Macromolecules
ARTICLE

Gas Phase Polymerization of Ethylene with Supported α-Diimine Nickel(II) Catalysts

Marcus M. Wegner, Anna K. Ott, and Bernhard Rieger*

WACKER-Lehrstuhl für Makromolekulare Chemie, Technische Universität München Lichtenbergstrasse 4, D-85747 Garching, Germany

Received November 30, 2009; Revised Manuscript Received February 18, 2010

ABSTRACT: An efficient synthetic strategy for new 2,5- and 2,6-substituted unbridged and 1,4-dithiane bridged ligands is presented. The reaction of the latter compounds with $Ni(acac)_2$ and trityl tetrakis-(pentafluorophenyl)borate gave the corresponding Ni(II) complexes in high yields. The structure of one of these complexes was determined by X-ray analysis. These complexes were supported on silica without a chemical tether and were used as catalysts for ethylene polymerization reactions in the gas phase. Furthermore, ethylene was polymerized with the unsupported 2,5-complexes in homogeneous solution for comparison. The influence of the ligand structure, hydrogen and temperature on the polymerization performance was investigated. The supported catalysts showed moderate to high activities and produced polyethylenes ranging from HDPE to LLDPE, without further addition of an 1-olefin comonomer. In contrast to 2,6-complexes, which generate high molecular weight polyethylene, the 2,5-compounds afford materials of lower molecular weight comprising terminal and internal double bonds. In addition, video microscopy experiments allowed to investigate the growth of single polyethylene particles. Electron microscopy was applied to show that their morphology is a replicate of the starting catalyst grains.

Introduction

In the mid 1990s Brookhart introduced a new type of late transition metal catalysts for the polymerization of ethylene.[1] The α-diimine Ni(II) catalysts **1** and **1a** (Chart 1) are able to produce LLDPE-like ethylene homopolymers, which are comparable to polymers obtained by copolymerization of ethylene and higher α-olefins.[1,2]

The reason for that are isomerization reactions of the growing polymer chain end (chain walking).[3] Despite their versatile advantages, unfortunately, the activated catalysts **1** and **1a** deactivate rapidly in the presence of hydrogen. Recently, we reported on new polyaromatic, hydrogen-stable Ni(II) complexes, such as **2a** and **2b** (Chart 1).[4] In homogeneous solution polymerization they are highly active and ligand design allows a high precision in control of the microstructure and therefore on the properties of the resulting materials.

Most of the technical polyethylenes are produced in heterogeneous slurry or gas phase processes. To apply new single-site catalysts under industrial conditions as "drop-in systems" they have to be supported. Heterogenized catalysts should combine the advantages of the classical heterogeneous catalysis, such as good morphology, little reactor fouling, high powder density, with the advantages of the homogeneous reaction, such as high activity, control over the polymer microstructure and over molecular weight distribution.[5] Catalyst immobilization is still a great challenge, since fractionation of the catalyst has to take place in a controlled way in order to generate a homogeneous product morphology. Silica is mainly used as support for single-site catalysts due to its high surface area, good porosity and mechanical properties.[5,6] In literature various methods and carriers are described to support nickel diimine complexes. Neutral nickel complexes were supported on silica gel with and without MAO pretreatment and were used in slurry and gas phase processes.[7] Brookhart reported on covalently anchored complexes to enhance activity and prevent leaching from the surface.[8]

Chart 1. α-Diimine Nickel(II) Complexes

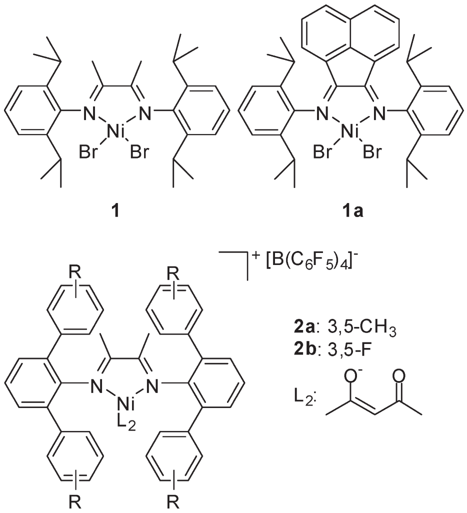

In contrast to metallocenes, α-diimine nickel catalysts can directly be supported on silica gel without decomposition due to the low oxophilicity of late transition metals. Silica-supported ionic diimine nickel complexes for gas phase polymerization have been reported by Eastman Chemical.[9] A chemical linkage is not required for gas phase polymerization, since leaching of the catalyst during the polymerization process in the gas phase is minimal or not existing.[10] Additionally, physically or chemically adsorbed compounds have the advantage that the structure of the complex has not to be changed by a linker and the original electronical and structural properties are maintained on the carrier.

Video microscopy is a new and powerful optical tool to observe the growth and fragmentation of polymer particles. A minireactor

---

*To whom all correspondence should be addressed. E-mail: rieger@tum.de.

Scheme 1. Synthesis of α-Diimine Nickel(II) Complexes

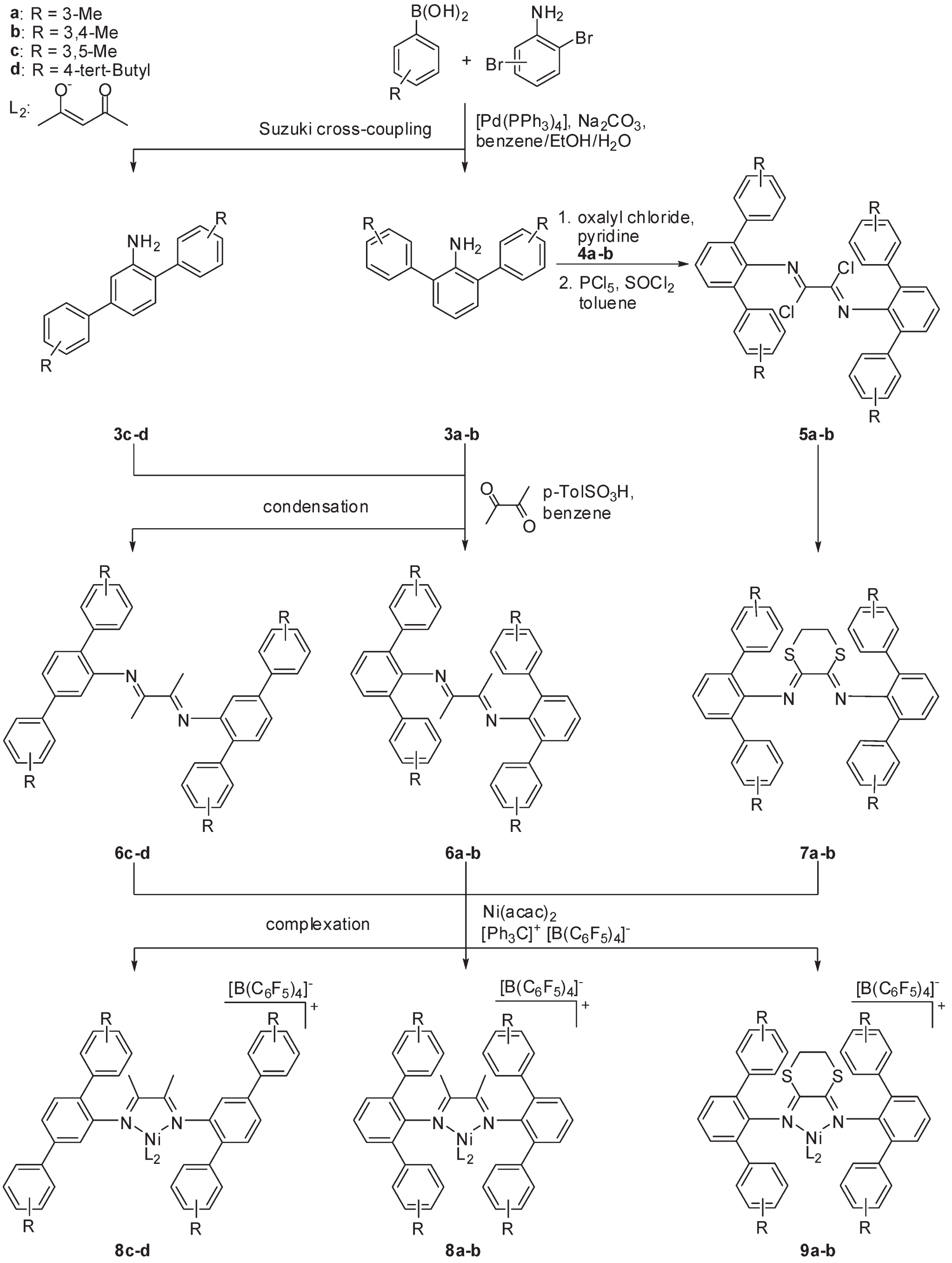

combined with a light microscope and a camera was first used for investigations on the polymerization of butadiene in the gas phase by Reichert et al.[11] Weickert and Fink et al. reported on polymerization with ethylene and propylene as well.[12,13]

One major objective to support single-site catalysts is to replicate the structure of the carrier into the morphology of the polymer particles. Electron microscopy is an appropriate method to characterize the structure and morphology of polymer particles.

Herein we present a synthetic route to 2,5- and 2,6-substituted polyaromatic α-diimine Ni(II) catalysts based on 2,3-butanedione as well as 1,4-dithiane-bridged 2,6-catalysts. These new compounds were directly supported on silica gel in order to polymerize ethylene in the gas phase. For comparative studies ethylene was polymerized using the unsupported 2,5-catalysts in toluene as well. We describe the influences of ligand structure and polymerization conditions on the polyethylene properties. Additionally, video and electron microscopy experiments allowed a detailed insight into particle forming processes.

Results and Discussion

Ligand and Complex Synthesis. The new α-diimine ligands based on 2,3-butanedione as well as the corresponding nickel(II) complexes can be obtained in an easy four step synthesis in very good yields (Scheme 1).[4,14]

The Grignard reaction with variably substituted bromobenzenes, followed by reaction with trimethylborate gave boronic acids in excellent yields. The latter compounds were converted to the corresponding terphenylamines **3a−d** by palladium-catalyzed Suzuki cross coupling reactions with 2,6-dibromoaniline and 2,5-dibromoaniline, respectively. The third step involved the formation of polyaromatic diimines by acid-catalyzed condensation with 2,3-butanedione.

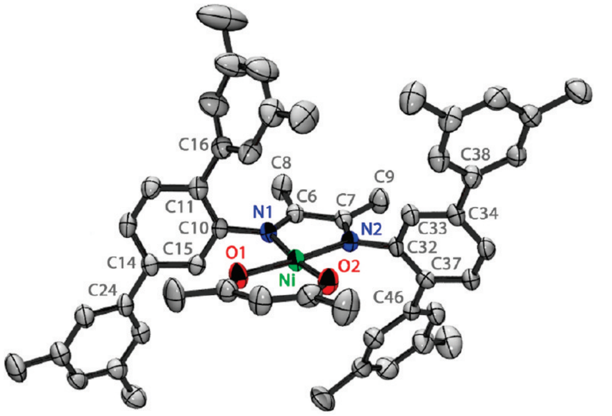

Figure 1. Pov-Ray image of octamethyl complex **8c**. Solvent molecules, hydrogen atoms, and the counterion are omitted for clarity. The atoms are drawn as 50% thermal ellipsoids. Selected bond lengths [Å]: Ni(1)−O(1) 1.819, Ni(1)−N(1) 1.887, N(1)−C(6) 1.281, N(2)−C(7) 1.290, C(6)−C(7) 1.492, N(1)−C(10) 1.441, and N(2)−C(32) 1.446. Selected bond angles [deg]: O(1)−Ni(1)−O(2) 95.07, N(1)−Ni(1)−N(2) 82.34, C(7)−N(2)−Ni(1) 115.9, C(6)−N(1)−Ni(1) 116.2, C(10)−C(11)−C(16) 124.3, C(15)−C(14)−C(24) 121.4, C(32)−C(37)−C(46) 122.5, and C(33)−C(34)−C(38) 119.6.

Complexation of the diimine ligands **6a−d** with the Ni(acac)$_2$ precursor and the trityl salt of $[B(C_6F_5)_4]^-$ led to red colored complexes **8a−d** in yields up to 85%.

A synthesis strategy to 1,4-dithiane-bridged diimines was successfully developed by modifying and improving literature procedures (Scheme 1).[9] First of all, oxalyl diamides **4a−b** were obtained from the reaction of 2,6-terphenylamines **3a−b** with oxalyl chloride. The reaction of the two chlorination agents PCl_5 and $SOCl_2$ with the oxalyl diamides at higher temperatures finally afforded the yellow bis-imidoyl chlorides **5a−b** in yields above 80%. The desired 1,4-dithiane-bridged diimines **7a−b** were subsequently obtained by reaction of bis-imidoyl chlorides **5a−b** with 1,2-ethanedithiol. The conversion to the Ni(II) complexes **9a−b** is according to **8a−b** reaching yields up to 92%.

Solid State Structure. In contrast to the highly symmetrical 2,6-α-diimine nickel(II) complexes, the 2,5-Ni(II) complexes **8c−d** can show in general two structural isomers. In case of **8d** there exists a mixture of two species. However, the ^{1}H NMR analysis of **8c** shows, in contrast to **8d**, only one isomer. Suitable crystals for X-ray analysis were obtained by slow condensation of pentane into the CH_2Cl_2 solution of complex **8c** at room temperature. The molecular structure of complex **8c** is illustrated in Figure 1.

The unit cell includes two complex molecules with counterions and two molecules of methylene chloride. The X-ray structure of **8c** exhibits a C_2 symmetry. Coordination around the nickel center is distorted square planar, as expected. The shift of one phenyl ring from the ortho to the meta position opens the area around the nickel center, hence, there is more space for an axial attack of a monomer and of course probability of β-hydride elimination reactions increases.

Heterogenization. The directly supported precatalysts were prepared using a slightly modified procedure from literature.[9] The silica gel SP9-496 from Grace-Davison was heated at 350 °C to remove all water from the surface. The reduced oxophilicity and therefore greater functional group tolerance of late transition metals allows heterogenization on silica gel. The desired amount of complex and silica gel were mixed in toluene. Removing the solvent led to red supported precatalysts. Even after several months no decomposition was observed, which would cause a change in color or modify the visual appearance. The amount of nickel was controlled by weighting, elemental analysis and in selected cases by ICP. The determined values are in the range of the theoretical calculated loadings (Table 1).

Table 1. Synthesized Precatalysts

complex	precatalyst	wt % Ni
8a	**10a**	1.0[a]
8a	**10a1**	0.24
8a	**10a2**	0.25[a]
8b	**10b**	1.0[a]
9a	**11a**	1.0[a]
9a	**11a1**	0.27
9b	**11b**	1.0[a]
8c	**10c**	1.0[a]
8d	**10d**	1.0[a]

[a] Theoretical maximum nickel loading.

Gas Phase Polymerization. The gas phase polymerization of ethylene was performed in a 450 mL steel autoclave in the presence of sodium chloride. Additional to the gas phase polymerization, ethylene was polymerized in toluene with the unsupported 2,5-catalysts for comparison. The optimal activator for polyaromatic α-diimine Ni(II) catalysts is TMA, which gives in solution at a Al/Ni ratio of 500 the highest activities.[4] For polymerization in the gas phase an increased aluminum concentration (Al/Ni = 1000) is required, since TMA can react with silanol groups on the surface. In general, activity values of a catalyst deeply depend on reactor type and reaction conditions as well as the considered polymerization time. In order to get more reliable and convincing results of activity the whole experiments were carried out for 1 h. It is noteworthy that all catalysts were active at 30 °C as well as 60 °C until the reaction was stopped. Polymerization conditions and results are summarized in Table 2.

A perfect particle forming process requires on the one hand homogeneous temperature distribution and on the other hand an uniform distribution of ethylene in the growing polymer particle.[15] The unsupported 2,6-catalysts are highly active in solution polymerization of ethylene which release a lot of heat. It should be mentioned that in some experiments at 30 °C temperature rose by 5 °C in the gas phase, which could create hot spots leading to inhomogeneities and therefore to a decrease in activity. The 2,6-catalysts exhibit the highest activities at 30 °C. **10b**, **11a**, and **11b** show their best performance in the presence of hydrogen. This is not surprising and can be explained by more homogeneous reaction conditions under hydrogen atmosphere. We previously reported on the same phenomena in solution polymerization.[14] The industrial interesting activity of 100 $kg_{PE}/g_{Ni}\cdot h$ and 1 $kg_{PE}/g_{het\ cat}$, respectively, is achieved by **10a**, **10b**, and **11a**. Elevated temperature (60 °C) results in an activity decline. Because of higher polymerization temperature less ethylene adsorbs on the particle surface and penetrates through the particle to the active center. Furthermore, heat removal from the particle must be considered as well. The sterically less demanding tetramethyl-substituted catalysts **10a** and **11a** show higher activities at 60 °C than the octamethyl-substituted analogues.

10a1 and **11a1** with 0.24 wt % Ni and 0.27 wt % Ni, respectively, exhibit slightly better activities at 60 °C than the higher loaded Ni(II) catalysts. A higher amount of nickel centers produce more heat which inhibits activity by insufficient removal. Another explanation is that not every nickel center is accessible for ethylene in case of the higher loaded catalysts. Generally, activity of supported

Table 2. Polymerization Results

entry	cat[a]	wt % Ni	sup. precat.[b] [mg]	temp. [°C]	X [m mmol H_2/ n mol C_2H_4]	yield [g]	g_{PE}/ $g_{het\ cat}$	kg_{PE}/ g_{Ni}/h	M_w[c] 10^{-3} [g/mol]	PDI[c]	branches/ 1000 C[d]	T_m[e] [°C]
1	**10a**	1.0	7.0	30	0	9.5	1357	136	2220	1.7	8	126.7
2	**10a**	1.0	8.5	30	1.92	9.9	1165	117	2300	1.7	8	126.8
3	**10a**	1.0	9.5	60	0	7.2	758	76	2510	2.0	12	120.2
4	**10a**	1.0	7.9	60	1.92	2.8	354	35	2460	1.9	12	121.7
5	**10a1**	0.24	18.9	30	0	5.8	307	127	3600	1.6	7	128.4
6	**10a1**	0.24	19.6	30	1.92	4.8	245	101	2240	1.9	8	128.7
7	**10a1**	0.24	19.3	60	0	4.4	228	94	3460	1.7	13	117.6
8	**10a1**	0.24	20.5	60	1.92	1.9	93	38	2910	2.0	12	119.9
9	**10b**	1.0	7.4	30	0	6.5	878	88	2310	1.8	9	124.1
10	**10b**	1.0	8.2	30	1.92	10.9	1329	133	1990	1.8	9	126.8
11	**10b**	1.0	8.9	60	0	2.5	281	28	2080	2.1	14	116.1
12	**10b**	1.0	7.2	60	1.92	1.0	139	14	2440	2.2	16	116.5
13	**11a**	1.0	7.7	30	0	3.1	403	40	2410	1.8	7	125.2
14	**11a**	1.0	7.6	30	1.92	8.1	1066	107	2690	1.8	8	126.0
15	**11a**	1.0	6.7	60	0	3.5	522	52	2100	1.8	16	117.7
16	**11a**	1.0	6.4	60	1.92	2.5	391	39	3700	1.9	14	118.5
17	**11a1**	0.27	28.0	30	0	5.2	186	69	3050	1.7	8	125.0
18	**11a1**	0.27	34.0	30	1.92	7.3	215	79	2810	1.9	8	125.3
19	**11a1**	0.27	31.0	60	0	6.5	210	77	2710	1.7	16	117.7
20	**11a1**	0.27	32.0	60	1.92	4.1	128	47	2060	1.9	15	118.2
21	**11b**	1.0	8.4	30	0	2.1	250	25	2900	2.1	9	126.7
22	**11b**	1.0	7.9	30	1.92	3.9	494	49	3820	1.6	8	123.3
23	**11b**	1.0	15.4	60	0	3.1	201	20	2980	2.0	18	107.2
24	**11b**	1.0	10.5	60	1.92	2.2	210	21	3420	1.7	16	111.9
25	**10c**	1.0	8.7	30	0	1.6	184	18	80.60	3.6	18	129.6
26	**10c**	1.0	8.3	30	3.84	2.2	265	27	86.90	2.9	17	132.5
27	**10c**	1.0	8.9	60	0	4.9	551	55	34.10	4.4	22	119.9
28	**10c**	1.0	7.0	60	3.84	5.8	829	83	35.80	3.4	30	120.8
29	**10d**	1.0	10.3	30	0	0.5	49	5	36.20	2.1	10	128.8
30	**10d**	1.0	8.9	30	3.84	0.4	45	5	53.40	4.1	15	129.7
31	**10d**	1.0	8.2	60	0	1.1	134	13	11.40	3.2	31	117.3
32	**10d**	1.0	9.2	60	3.84	0.4	43	4	11.80	2.9	28	116.8
Solution Polymerization[f]												
33	**8c**		7.4	30	0	88.7		302	14.10	3.3	6	133.0
34	**8c**		7.4	30	3.84	58.8		201	14.40	2.3	20	130.4
35	**8c**		7.4	60	0	39.2		134	3.50	2.1	25	111.8
36	**8c**		7.4	60	3.84	58.4		199	3.20	2.3	23	111.7
37	**8d**		16.0	30	0	80.4		137	8.10	2.8	8	125.3
38	**8d**		16.0	30	3.84	81.3		139	7.85	2.9	10	126.3
39	**8d**		16.0	60	0	46.8		80	2.60	2.4	31	107.1
40	**8d**		16.0	60	3.84	41.9		71	2.57	2.4	29	107.6

[a] Cocatalyst: TMA. Al/Ni = 1000 (gas phase). Polymerization time: 1 h. Ethylene pressure: 10 bar. [b] For the solution polymerization the amount of unsupported catalyst is mentioned. [c] Molecular weights and polydispersities are determined by GPC. [d] The branching degree was determined by ^{1}H NMR. [e] Melting points were determined by DSC. [f] Cocatalyst: TMA. Al/Ni = 500, 800 mL toluene. Polymerization time: 1 h. Ethylene pressure: 10 bar.

catalysts reaches a limiting value with increasing catalyst loading.

The 2,5-catalysts show a different behavior of activity. In the gas phase the highest activities are obtained at 60 °C, but in solution the maxima of activity are achieved at 30 °C (Figure 2).

It is suggested that different mass transport (ethylene) and/or heat transfer limitations through the lower molecular weight polyethylene produced by these catalysts (see below) arise.

Unfortunately, heterogenization of the 2,5-complexes leads to a decline in activity, which is a well-known effect for supported single-site catalysts. However, **10c** achieves a remarkable activity of 83 $kg_{PE}/g_{Ni} \cdot h$ at 60 °C which is slightly lower compared to **8c**.

Surprisingly, activities of **8c**, **8d** in solution and **10c**, **10d** in the gas phase remain constant or are actually higher in the presence of hydrogen. Usually the activity drops in the presence of hydrogen. A similar behavior was observed for $LFeCl_2$ systems.[16] The mechanism as proposed by Zharakov et al. is used to explain this hydrogen activation effect.[17] The ethylene polymers of 2,5-complexes have a broader molecular weight distribution and a high percentage of terminal vinyl groups (see below). A small amount of low molecular weight products are produced and incorporated by 2,1-insertion into the polymer chain, whereas dormant species are formed. Hydrogen converts this species via chain transfer reaction into a polymerization active hydride. Therefore, the

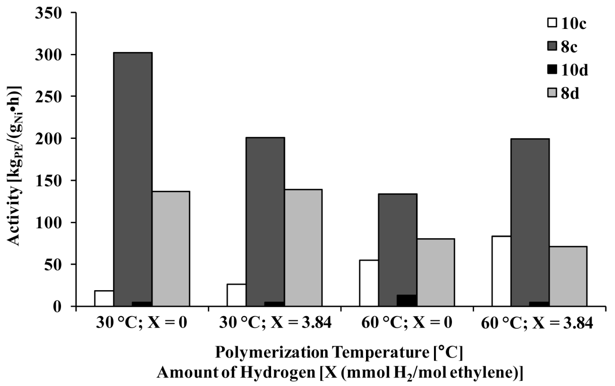

Figure 2. Activity values of 2,5-catalysts in the gas phase (**10c**, **10d**) and in solution (**8c**, **8d**).

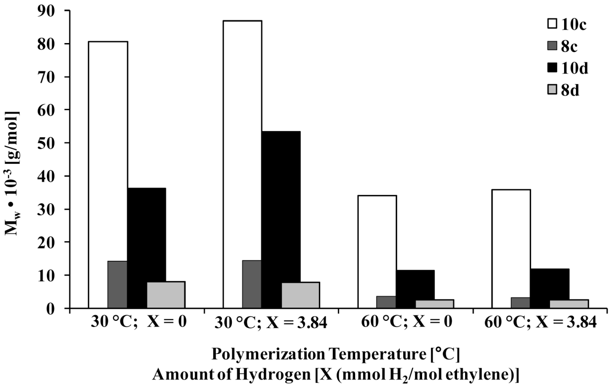

Figure 3. Molecular weights of the polyethylenes obtained by 2,5-catalysts in the gas phase (**10c**, **10d**) and in solution (**8c**, **8d**).

overall concentration of active sites is increased and hence the activity rises.

All four 2,6-catalysts produce high molecular weight polyethylenes with M_W > 1 000 000 g/mol. No significant influence of temperature and to our surprise hydrogen could be detected. This is in contrast to published results of homogeneous polymerization reactions.[4] We would expect lower molecular weights with an increasing amount of hydrogen as we observed in homogeneous solution experiments. It is suggested that only a lesser amount of hydrogen is located at the active centers because of adsorption and mass transport limitations. The polydispersity index of the polyethylenes was around 2, which is typical for single-site-compounds.

Compared to 2,6-complexes, 2,5-catalysts produce polyethylene with lower molecular weight up to 100 000 g/mol (Figure 3).

This difference is attributed to the more open active center due to shifting one phenyl ring from the ortho to the meta position which is underlined by the crystal structure of **8c**. Chain termination happens more often compared to the "close"-2,6 species. Thus, the resulting molecular weights of the polyethylene are significantly reduced. Hydrogen has no detectable influence on molecular weight in the gas phase as well as in solution. However, ligand design affects molecular weight of the polymers. The 3,5-substituted catalysts **8c** and **10c** better prevent chain termination reaction and therefore produce polyethylenes with higher molecular weight than in the case of **8d** and **10d**. Compared to solution polymerization, notable higher molecular weight polymers are produced by the 2,5-catalysts in the gas phase. The increasing molecular weights lead to higher melting points of the polymers in the gas phase. Similar results reported by Janiak and Rieger with metallocenes and by Basset with diimine nickel complexes.[7d,18] The higher molecular weights can be explained by reduced chain termination and/or higher chain propagation. The surface of the carrier reduces the space around the active center and might decrease chain transfer rates as well. Furthermore, the elevated values may be attributed to chain shuttling polymerization reactions on the surface.[19] The transfer of polymer chains from one catalyst via trimethylaluminum to another active center can also cause longer polymer chains. The 2,5-catalysts show slightly higher unimodal molecular weight distributions ranging between 2 and 4.

The nickel diimine catalysts have the remarkable ability to produce branched polyethylene from ethylene alone. A β-hydride elimination generates a vinyl-terminated polymer chain. Rotation around the double bond and 2,1-insertion of a ethylene molecule results in methyl-branched polymer. A number of repeated isomerization reactions lead to longer branched polymers. At ambient temperature (30 °C) the branching degree of all polyethylenes obtained from the 2,6-catalysts is below 1% which results in almost linear polyethylene. The ligand structure has no influence on the degree of branching, but there is a small trend in melting points. At higher temperatures chain isomerization becomes more favorable. Two main trends can be seen. The more bulky the ligand the faster isomerization reactions occur and therefore the extent of branching increases whereas melting temperature declines. It seems that the introduction of an additional backbone (**11a**) or a methyl-group (**10b**) have a similar influence on polymer properties. The most sterical catalyst **11b** exhibits the highest branching degree and the lowest melting points, as expected (Figure 4).

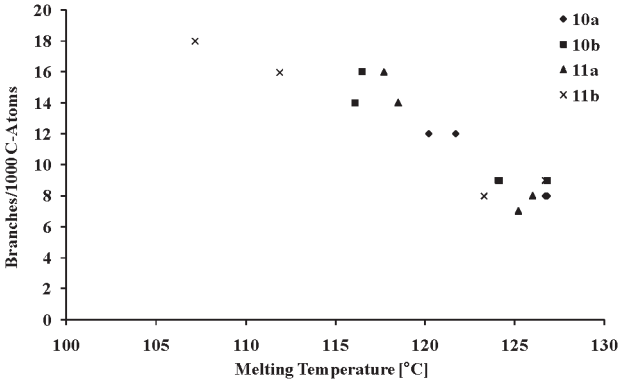

Figure 4. Melting temperature vs branches.

The 2,5-catalysts produce polyethylene with a branching degree between 1 and 3%. The highest values are detected at 60 °C. No significant influence of carrier as well as of ligand structure on the isomerization behavior could be observed. These new polymers bear double bonds. The ^{1}H NMR spectra of polyethylenes produced by 2,5-catalysts record three additional peaks in the olefin region in agreement with vinyl- and vinylen groups. Figure 5 shows a representative spectrum.

The two signals 1 and 3 are assigned to the protons of a vinyl end group. The broader peak at 5.4 ppm is attributed to a vinylene fragment. Signal 4 belongs to methylene groups next to a double bond.

Particle Morphology. The major objective of heterogenization is replication of support morphology into the final polymer. Figure 6 depicts polymer particles from gas phase polymerization.

The images in Figure 6 show spherical structures. However, sodium chloride affects the polymer morphology by acting as an abrasive. Therefore, to gain information on the growth and the formation of polymer particles without the influence of sodium chloride, single particles of **10a2** were analyzed by video microscopy. Figure 7 shows images after different polymerization times.

All observed particles were active during the polymerization, but there were differences in the growth of individual grains. Without the grinding effect of sodium chloride the structure and the morphology of polymer particles remained a replicate of the starting catalyst particles.

Electron microscopy studies of these structures were performed to gain a deeper insight into structure formation. It is obvious from Figure 8 that the porous structure of the silica gel remains in the polymer particles as well.

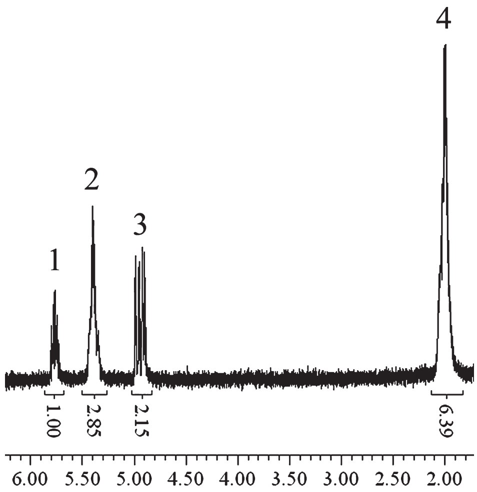

Figure 5. Representative ^{1}H NMR spectrum of the polyethylenes obtained by 2,5-catalysts. Labels are discussed in the text.

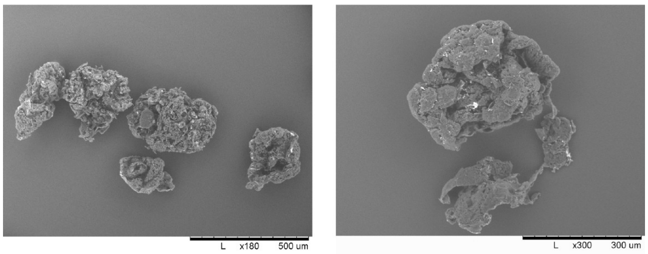

Figure 6. Representative polymer particles made by gas phase polymerization.

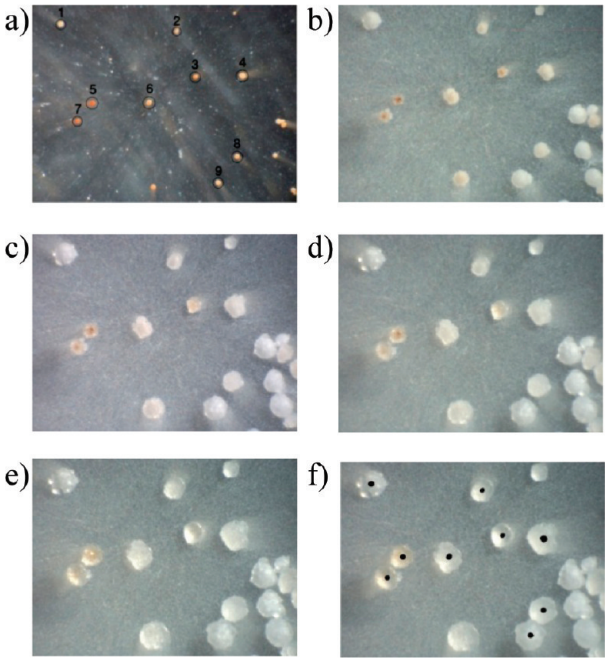

Figure 7. Snapshots of catalyst **10a2** and growing polymer particles after (a) 0, (b) 20, (c) 40, (d) 60, (e) 90, and (f) 120 min at 60 °C and 4 bar ethylene pressure.

The cauliflower-like morphology consists of subparticles which are held together by polymer fibers. The polymer particles are not a compact material. The inside consists of pores which allow diffusion of ethylene to the active centers (Figure 9).

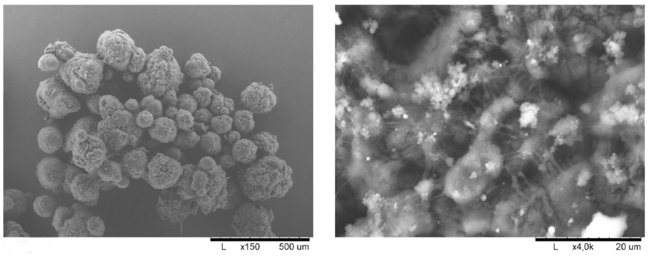

Figure 8. SEM images of polymer particles produced by **10a2**.

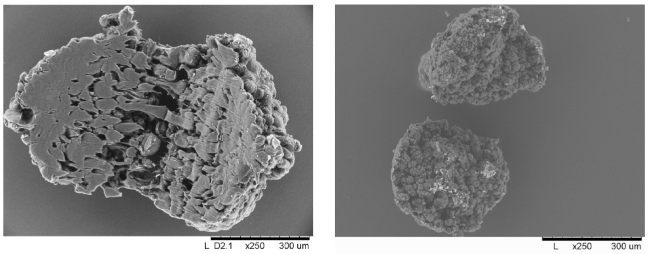

Figure 9. SEM images of the cross-section of polymer particles.

Conclusion

New Ni(II) complexes bearing 2,5- (**8c**, **8d**) as well as 2,6-substituted (**8a**, **8b**, **9a**, **9b**) diimine ligands are efficiently prepared by an optimized and high yielding route. These complexes were supported on silica gel and successfully used as a new catalyst type to perform polymerization of ethylene in the gas phase under various conditions. Additionally, ethylene was polymerized with the unsupported 2,5-catalysts for comparison. Partially the supported catalysts show high activities above 100 $kg_{PE}/g_{Ni}\cdot h$ and 1 $kg_{PE}/g_{het\ cat}$, respectively. The 2,6-catalysts produce polyethylenes with molecular weights over 10^6 g/mol whereas the 2,5-catalysts generate lower molecular polymers below 100 000 g/mol. Polyethylenes produced in the gas phase reveal higher molecular weights than those from solution. The microstructure as well as the melting behavior of the polyethylenes could be controlled and tailor-made by ligand design. Moreover, vinyl and vinylene groups were realized by using 2,5-catalysts. Video microscopy experiments show that the polymers replicate the morphology of the catalyst particles.

The polyaromatic α-diimine nickel(II) complexes have not yet reached their full potential. Expecially the polyethylenes of the 2,5-catalysts are characterized by internal and terminal double bonds. Therefore, the polymers can be chemically modified and functionalized.

Experimental Section

General Procedures. All air- and moisture-sensitive adjustments were carried out under dry argon atmosphere, using conventional Schlenk techniques. For purification, methylene chloride was distilled from CaH_2, *n*-pentane from sodium and toluene from $LiAlH_4$. Pyridine was dried over activated aluminum oxide. Diacetylacetonatonickel(II), phosphorus pentachloride, thionyl chloride, sodium chloride, 2,5- and 2,6-dibromoaniline were purchased from Merck and ABCR and used as received. Ethylene (Linde, grade 3.0) and hydrogen (Linde, grade 5.0) were used without further purification. Silica gel SP9−496 was supplied by Grace Davison. The synthesized compounds were characterized by ^{1}H- and ^{13}C NMR analysis on a Bruker DRX 400 and on a Bruker ARX-300 spectrometer. Chemical shifts δ are given in ppm in reference to ^{1}H NMR and ^{13}C NMR signals of the deuterated solvents. MALDI-TOF and CI mass-spectra were recorded on Bruker Daltonics REFLEX III and Finnigan MAT TSQ-7000 mass spectrometers in the

Department of Mass Spectrometry, University of Ulm and on Bruker Biflex III (MALDI-TOF) in the Microanalytical Department of Inorganic Chemistry, TU München. Elemental analyses (C, H, N) of the compounds were determined in the Microanalytical Laboratory of the University of Ulm, TU München and outside the university. The ICP analysis was performed outside the university. The X-ray diffraction measurement was performed at the University of Ulm on a Rigaku AFC7S diffractometer. $[Pd(PPh_3)_4]$, trityl tetrakis(pentafluorophenyl)borate and the different boronic acids were prepared according to published literature procedures.

The polymers were analyzed by NMR spectroscopy in bromobenzene-d_5 and *p*-xylene-d_6 at 363 K by using a Bruker AMX-500 spectrometer. The amount of branches was determined by ^1H NMR spectroscopy. Molecular weights and distributions were measured using a Waters Alliance GPC 2000 system (145 °C, 1,2,4-trichlorobenzene) relative to polystyrene standards. Melting points were determined by differential scanning calorimetry (DSC). The melting curves were recorded on a Perkin−Elmer DCS-7. Scanning electron microscopy images were taken on a Hitachi Tabeltop Microscope TM-1000. Gas phase polymerization experiments were performed in a 450 mL and solution polymerization in 2 L Parr autoclave. Ethylene and hydrogen were constantly fed to the reactor at constant pressure. Gas flows were recorded with the software Genie V 3.0. Addition of hydrogen was controlled by a master-slave setup.

General Procedure for Synthesis of the Terphenylamines. The terphenylamines were synthesized by previously reported literature procedures.[4,14] In a 1 L Schlenk flask dibromoaniline (1 equiv), $[Pd(PPh_3)_4]$ (12 mol %), 2 M Na_2CO_3 solution (6.75 equiv) were dissolved in benzene (400 mL). Solution of an arylboronic acid (2.6 equiv) in ethanol (50 mL) was added and stirred under reflux for 48 h (2,5-terphenylamines) and 72 h (2,6-terphenylamines), respectively. The organic phase was separated and the aqueous phase was extracted with benzene. The combined organic phases were treated with hydrochloric acid (25 mL). The solvent was removed and the residue was suspended with diethyl ether. Saturated Na_2CO_3-solution was added and the mixture was stirred for 10 min. The organic phase was separated and the aqueous phase was extracted with diethyl ether. The organic solvent was removed in vacuo. The crude product was recrystallized from methanol to give pure white terphenylamines.

3,3″-Dimethyl-1,1′;3′,1″-terphenyl-2′-ylamine (3a). 3-Methylphenylboronic acid (28.9 g, 212.6 mmol); 2,6-dibromoaniline (20.5 g; 81.7 mmol); $[Pd(PPh_3)_4]$ (11.3 g, 9.8 mmol); Na_2CO_3 (58.5 g, 551.5 mmol); white solid; yield: 18.1 g (81%). ^1H NMR (400.13 MHz, $C_2D_2Cl_4$, 298 K) δ: 7.47−7.49 (m, 6H, H_{arom}), 7.31 (d, 2H, H_{arom}), 7.26 (d, 2H, H_{arom}), 7.00 (t, 1H, H_{arom}), 4.02 (s, 2H, NH_2), 2.55 (s, 6H, CH_3). ^{13}C NMR (100.16 MHz, $C_2D_2Cl_4$, 298 K) δ: 140.89, 139.81, 138.57, 130.10, 129.73, 128.84, 128.08, 127.92, 126.36, 118.4, 21.67. Anal. Calcd for $C_{20}H_{19}N$: C, 87.87; H, 7.01; N 5.12. Found: C, 87.71; H, 6.99; N, 5.07.

3,4,3″,4″-Tetramethyl-1,1′;3′,1″-terphenyl-2′-ylamine (3b). 3,4-Dimethylphenylboronic acid (34.7 g, 231.3 mmol), 2,6-dibromoaniline (22.3 g, 88.9 mmol), $[Pd(PPh_3)_4]$ (13.8 g, 11.9 mmol), Na_2CO_3 (63.6 g, 600.1 mmol); white solid; yield: 16.5 g (62%). ^1H NMR (400.13 MHz, $C_2D_2Cl_4$, 298 K) δ: 7.52 (s, 2H, H_{arom}), 7.48 (d, 2H, H_{arom}), 7.42 (d, 2H, H_{arom}), 7.32 (d, 2H, H_{arom}), 7.04 (t, 1H, H_{arom}), 4.12 (s, 2H, NH_2), 2.53 (s, 6H, CH_2), 2.52 (s, 6H, CH_3). ^{13}C NMR (100.16 MHz, $C_2D_2Cl_4$, 298 K) δ: 141.01, 137.43, 137.09, 135.51, 130.58, 130.19, 129.60, 127.91, 126.71, 118.13, 19.97, 19.63. Anal. Calcd for $C_{22}H_{23}N$: C, 87.66; H, 7.69; N, 4.65. Found: C, 87.61; H, 7.67; N, 4.68.

3,5,3″,5″-Tetramethyl-1,1′;4′,1″-terphenyl-2′-ylamine (3c). 3,5-Dimethylphenylboronic acid (25.0 g, 166.7 mmol), 2,5-dibromoaniline (16.1 g, 64.2 mmol), $[Pd(PPh_3)_4]$ (8.9 g, 7.7 mmol), Na_2CO_3 (45.9 g, 433.1 mmol); white solid; yield: 16.3 g (84%). ^1H NMR (400.13 MHz, $C_2D_2Cl_4$, 298 K) δ: 7.32 (s, 2H, H_{arom}), 7.27 (d, 1H, H_{arom}), 7.20 (s, 2H, H_{arom}), 7.13 (dd, 1H, H_{arom}), 7.08 (s, 2H, H_{arom}), 7.05 (ds, 1H, H_{arom}), 3.96 (s, 2H, NH_2), 2.47 (s, 6H, CH_3), 2.46 (s, 6H, CH_3). ^{13}C NMR (100.16 MHz, $C_2D_2Cl_4$, 298 K) δ: 143.73, 141.20, 140.88, 139.14, 138.48, 138.27, 130.85, 129.06, 128.93, 126.86, 126.82, 125.02, 117.65, 114.26, 21.60, 21.55. Anal. Calcd for $C_{22}H_{23}N$: C, 87.66; H, 7.69; N, 4.65. Found: C, 87.50; H, 7.67; N, 4.62.

4,4″-Di-*tert*-butyl-1,1′;4′,1″-terphenyl-2′-ylamine (3d). 4-t-Butylphenylboronic acid (27.0 g, 151.7 mmol), 2,5-dibromoaniline (14.6 g, 58.2 mmol), $[Pd(PPh_3)_4]$ (8.1 g, 7.0 mmol), Na_2CO_3 (41.6 g, 392.5 mmol); white solid; yield: 14.1 g (68%). ^1H NMR (400.13 MHz, $C_2D_2Cl_4$, 298 K) δ: 7.60 (d, 2H, H_{arom}), 7.46−7.52 (q, 6H, H_{arom}), 7.24 (d, 1H, H_{arom}), 7.11 (dd, 1H, H_{arom}), 7.03 (ds, 1H, H_{arom}), 3.92 (s, 2H, NH_2), 1.41 (s, 9H, CH_3), 1.40 (s, 9H, CH_3). ^{13}C NMR (100.16 MHz, $C_2D_2Cl_4$, 298 K) δ: 150.36, 150.10, 143.89, 140.71, 137.63, 136.01, 130.99, 128.66, 126.56, 126.46, 125.86, 125.78, 117.45, 113.99, 34.60, 34.55, 31.50. Anal. Calcd for $C_{26}H_{31}N$: C, 87.34; H, 8.74; N, 3.92. Found: C, 87.22; H, 8.59; N, 3.90.

General Procedure for Synthesis of the α-Diimines Based on 2,3-Butanedione. The diimines were prepared according to literature procedures.[4,14] In a 250 mL Schlenk flask the terphenylamine (2.2 equiv) and a catalytic amount of *p*-toluenesulfonic acid monohydrate (0.06 equiv) were dissolved in benzene (150 mL). 2,3-Butanedione (1 equiv) was added at once and a Dean−Stark apparatus attached. After refluxing the mixture for 48 h (2,5-terphenylamines) and 72 h (2,6-terphenylamines), respectively, the solvent was evaporated in vacuo. The crude product was taken up in methylene chloride followed by addition of methanol. The resultant yellow precipitate was filtered off and the precipitation procedure repeated two more times. The pure product was dried in vacuo to give a fine yellow powder.

$ArN{=}C(CH_3){-}C(CH_3){=}NAr$ (6a, Ar = 2,6-(3-$(CH_3)C_6H_4)_2$-C_6H_3). Terphenylamine **3a** (4.5 g, 16.5 mmol), 2,3-butanedione (646 mg, 7.5 mmol), *p*-TosOH·H_2O (86 mg, 0.45 mmol); yellow solid; yield: 3.6 g (80%). ^1H NMR (400.13 MHz, $C_2D_2Cl_4$, 298 K) δ: 7.30 (d, 4H, H_{arom}), 7.21 (t, 2H, H_{arom}), 7.14 (s, 4H, H_{arom}), 7.00−7.06 (m, 12H, H_{arom}), 2.20 (s, 12H, CH_3), 1.46 (s, 6H, CH_3). ^{13}C NMR (100.16 MHz, $C_2D_2Cl_4$, 298 K) δ: 166.29, 146.43, 139.49, 136.94, 130.93, 129.88, 129.39, 127.75, 127.72, 125.95, 124.24, 21.47, 16.01. Anal. Calcd for $C_{44}H_{40}N_2$: C, 88.55; H, 6.76; N, 4.69. Found: C, 88.41; H, 6.74; N, 4.64.

$ArN{=}C(CH_3){-}C(CH_3){=}NAr$ (6b, Ar = 2,6-(3,4-$(CH_3)_2C_6H_3)_2$-C_6H_3). Terphenylamine **3b** (6.0 g, 19.9 mmol), 2,3-butanedione (779 mg, 9.0 mmol), *p*-TosOH·H_2O (103 mg, 0.54 mmol); yellow solid; yield: 2.8 g (47%). ^1H NMR (400.13 MHz, $C_2D_2Cl_4$, 298 K) δ: 7.31 (d, 4H, H_{arom}), 7.21 (t, 2H, H_{arom}), 7.17 (s, 4H, H_{arom}), 6.91 (s, 8H, H_{arom}), 2.32 (s, 12H, CH_3),), 2.21 (s, 12H, CH_3), 1.55 (s, 6H, CH_3). ^{13}C NMR (100.16 MHz, $C_2D_2Cl_4$, 298 K) δ: 167.47, 145.95, 137.46, 135.86, 134.66, 131.23, 130.51, 129.04, 128.50, 126.41, 124.15, 19.74, 16.85. Anal. Calcd for $C_{48}H_{48}N_2$: C, 88.30; H, 7.41; N, 4.29. Found: C, 88.24; H, 7.40; N, 4.27.

$ArN{=}C(CH_3){-}C(CH_3){=}NAr$ (6c, Ar = 2,5-(3,5-$(CH_3)_2C_6H_3)_2$-C_6H_3). Terphenylamine **3c** (5.1 g, 16.9 mmol), 2,3-butanedione (662 mg, 7.7 mmol), *p*-TosOH·H_2O (88 mg, 0.46 mmol); yellow solid; yield: 4.1 g (82%). ^1H NMR (400.13 MHz, $C_2D_2Cl_4$, 298 K) δ: 7.50 (d, 2H, H_{arom}), 7.44 (dd, 2H, H_{arom}), 7.32 (s, 4H, H_{arom}), 7.06 (br. s, 6H, H_{arom}), 6.99 (ds, 2H, H_{arom}), 6.90 (s, 2H, H_{arom}), 2.43 (s, 12H, CH_3), 2.26 (s, 12H, CH_3), 1.92 (s, 6H, CH_3). ^{13}C NMR (100.16 MHz, $C_2D_2Cl_4$, 298 K) δ: 167.86, 148.84, 140.53, 140.28, 138.81, 138.47, 138.24, 130.66, 129.97, 128.60, 128.49, 127.00, 124.98, 122.99, 117.01, 21.63, 21.42, 16.23. Anal. Calcd for $C_{48}H_{48}N_2$: C, 88.30; H, 7.41; N, 4.29. Found: C, 88.13; H, 7.32; N, 4.22.

$ArN{=}C(CH_3){-}C(CH_3){=}NAr$ (6d, Ar = 2,5-(4-$(C(CH_3)_3)$-$C_6H_4)_2C_6H_3$). Terphenylamine **3d** (4.6 g, 12.9 mmol), 2,3-butanedione (504 mg, 5.9 mmol), *p*-TosOH·H_2O (67 mg, 0.35 mmol); yellow solid; yield: 3.1 g (69%). ^1H NMR (400.13 MHz, $C_2D_2Cl_4$, 298 K) δ: 7.63 (d, 4H, H_{arom}), 7.49−7.54 (m, 8H, H_{arom}), 7.36 (br. s, 8H, H_{arom}), 6.96 (ds, 2H, H_{arom}), 2.01 (s, 6H, CH$_3$), 1.40 (s, 18H, CH$_3$), 1.36 (s, 18H, CH$_3$). ^{13}C NMR (100.16 MHz, C$_2$D$_2$Cl$_4$, 298 K) δ: 168.35, 150.70, 149.89, 148.64, 140.08, 137.18, 135.99, 130.68, 130.22, 128.92, 126.62, 125.94, 124.84, 122.88, 117.07, 34.59, 34.54, 31.50, 16.54. Anal. Calcd for C$_{56}$H$_{64}$N$_2$: C, 87.91; H, 8.43; N, 3.66. Found: C, 87.75; H, 8.36; N, 3.66.

General Procedure for Synthesis of the Oxalyl Diamides. The desired terphenylamine (2.1 equiv) was dissolved in dry pyridine (40 mL) in a Schlenk flask and the stirred solution was treated under argon atmosphere dropwise with oxalyl chloride (1 equiv) at 0 °C. After the addition was finished the cooling was abandoned and the reaction mixture was allowed to stir for 12 h. Water was added and the solution was extracted with methylene chloride. The solvent was removed in vacuo and the crude product recrystallized from isopropanol to give a pure white oxalyl diamide product.

ArNC(O)−C(O)NAr (4a, Ar = 2,6-(3-(CH$_3$)C$_6$H$_4$)$_2$C$_6$H$_3$). Terphenylamine **3a** (3.2 g, 11.7 mmol), oxalyl chloride (0.70 g, 5.5 mmol); white solid; yield: 2.2 g (67%). ^{1}H NMR (400.13 MHz, C$_2$D$_2$Cl$_4$, 298 K) δ: 8.48 (s, 2H, NH), 7.46 (t, 2H, H$_{\mathrm{arom}}$), 7.38 (d, 4H, H$_{\mathrm{arom}}$), 7.19−7.25 (m, 8H, H$_{\mathrm{arom}}$), 7.16 (s, 4H, H$_{\mathrm{arom}}$), 7.06 (d, 4H, H$_{\mathrm{arom}}$), 2.40 (s, 12H, CH$_3$). ^{13}C NMR (100.16 MHz, C$_2$D$_2$Cl$_4$, 298 K) δ: 157.32, 139.75, 138.89, 138.04, 129.96, 129.45, 129.33, 128.29, 128.9, 127.94, 125.34, 21.64. Anal. Calcd for C$_{42}$H$_{36}$N$_2$O$_2$: C, 83.97; H, 6.04; N, 4.66. Found: C, 83.74; H, 6.18; N, 4.55.

ArNC(O)−C(O)NAr (4b, Ar = 2,6-(3,4-(CH$_3$)$_2$C$_6$H$_3$)$_2$C$_6$H$_3$). Terphenylamine **3b** (5.2 g, 17.3 mmol), oxalyl chloride (1.05 g, 8.3 mmol); white solid; yield: 3.5 g (64%). ^{1}H NMR (400.13 MHz, C$_2$D$_2$Cl$_4$, 298 K) δ: 8.51 (s, 2H, NH), 7.42 (t, 2H, H$_{\mathrm{arom}}$), 7.35 (d, 4H, H$_{\mathrm{arom}}$), 7.13 (s, 4H, H$_{\mathrm{arom}}$), 7.05 (d, 4H; H$_{\mathrm{arom}}$), 6.98 (d, 4H, H$_{\mathrm{arom}}$), 2.33 (s, 12 H, CH$_3$), 2.29 (s, 12H, CH$_3$). ^{13}C NMR (100.16 MHz, C$_2$D$_2$Cl$_4$, 298 K) δ: 157.60, 139.46, 136.74, 136.57, 135.71, 130.07, 129.92, 129.39, 129.30, 127.85, 125.59, 19.93, 19.74. Anal. Calcd for C$_{46}$H$_{44}$N$_2$O$_2$: C, 84.11; H, 6.75; N, 4.26. Found: C, 83.14; H, 6.77; N, 4.21.

General Procedure for Synthesis of the Bis(imidoyl) Chlorides. The oxalyl diamide (1 equiv), PCl$_5$ (2 equiv), and SOCl$_2$ (4 equiv) were solved in dry toluene (30 mL) and heated 1 h at 60 °C. The reactions mixture was cooled down to room temperature and pentane was slowly added to the stirred solution resulting in product precipitation. The precipitate was separated, washed with pentane and dried in vacuo. The product was isolated as a yellow powder.

ArN=C(Cl)−C(Cl)=NAr (5a, Ar = 2,6-(3-(CH$_3$)C$_6$H$_4$)$_2$C$_6$H$_3$). Oxalyl diamide **4a** (3.5 g, 5.8 mmol), PCl$_5$ (2.4 g, 11.5 mmol), and SOCl$_2$ (2.8 g, 23.5 mmol) were used; yellow solid; yield: 3.0 g (81%). ^{1}H NMR (400.13 MHz, C$_2$D$_2$Cl$_4$, 298 K) δ: 7.32−7.40 (m, 6H, H$_{\mathrm{arom}}$), 7.05−7.15 (m, 16H, H$_{\mathrm{arom}}$), 2.21 (s, 12H, CH$_3$).^{13}C NMR (100.16 MHz, C$_2$D$_2$Cl$_4$, 298 K) δ: 142.11, 138.31,137.41, 137.30, 131.38, 129.82, 129.40, 128.22, 127.98, 126.05, 125.91, 21.44. Anal. Calcd for C$_{42}$H$_{34}$Cl$_2$N$_2$: C, 79.11; H, 5.37; N, 4.39. Found: C, 78.88; H, 5.47; N, 4.34.

ArN=C(Cl)−C(Cl)=NAr (5b, Ar = 2,6-(3,4-(CH$_3$)$_2$C$_6$H$_3$)$_2$-C$_6$H$_3$). Oxalyl diamide **4b** (2.3 g, 3.50 mmol), PCl$_5$ (1.5 g, 7.2 mmol), and SOCl$_2$ (1.6 g, 13.45 mmol) were used; yellow solid; yield: 2.07 g (85%). ^{1}H NMR (400.13 MHz, C$_2$D$_2$Cl$_4$, 298 K) δ: 7.31−7.40 (m, 6H, H$_{\mathrm{arom}}$), 7.13 (s, 4H, H$_{\mathrm{arom}}$), 6.96−7.02 (m, 8H, H$_{\mathrm{arom}}$), 2.29 (s, 12H, H$_{\mathrm{arom}}$), 2.18 (s, 12H, H$_{\mathrm{arom}}$). ^{13}C NMR (100.16 MHz, C$_2$D$_2$Cl$_4$, 298 K) δ: 141.58, 137.59, 136.22, 136.13, 135.34, 131.76, 130.53, 129.40, 129.31, 126.33, 125.99, 19.73, 19.71. Anal. Calcd for C$_{46}$H$_{42}$Cl$_2$N$_2$: C, 79.64; H, 6.10; N, 4.04. Found: C, 79.52; H, 6.07; N, 3.88.

General Procedure for Synthesis of the 1,4-Dithiane-Bridged Diimines. 1,2-Ethanedithiol (5 equiv) was slowly added to a stirred solution of NaH (5 equiv) in dry THF (100 mL) at 0 °C. Cooling was abandoned and the reaction mixture was allowed to stir at room temperature for 2 h. Then bis(imidoyl) chloride (1 equiv) in dry THF (20 mL) was slowly added. The yellow solution was heated under reflux for 48 h. Water was added and extracted with methylene chloride. The solvent was removed in vacuo. The crude product was taken up in methylene chloride followed by addition of methanol. The resultant yellow precipitate was filtered off and the precipitation procedure repeated two more times. The pure product was dried in vacuo to give a fine yellow powder.

ArN=C(S(CH$_2$)$_2$S)C=NAr (7a, Ar = 2,6-(3-(CH$_3$)C$_6$H$_4$)$_2$-C$_6$H$_3$). Bis(imidoyl) chloride **5a** (2.0 g, 3.1 mmol), 1,2-ethanedithiol (1.48 g, 15.7 mmol), and NaH (377 mg, 15.7 mmol) were used; yellow solid; yield: 1.25 g (60%). ^{1}H NMR (400.13 MHz, C$_2$D$_2$Cl$_4$, 298 K) δ: 7.44 (d, 4H, H$_{\mathrm{arom}}$), 7.28 - 7.35 (m, 10H, H$_{\mathrm{arom}}$), 7.20 (t, 4H, H$_{\mathrm{arom}}$), 7.08 (d, 4H, H$_{\mathrm{arom}}$), 2.26 (s, 12H, H$_{\mathrm{arom}}$), 2.01 (s, 4H, CH$_2$). ^{13}C NMR (100.16 MHz, C$_2$D$_2$Cl$_4$, 298 K) δ: 153.91, 144.94, 139.02, 137.01, 131.23, 130.55, 129.26, 127.73, 127.48, 126.76, 124.97, 30.39, 21.51. Anal. Calcd for C$_{44}$H$_{38}$N$_2$S$_2$: C, 80.20; H, 5.81; N, 4.25. Found: C, 80.05; H, 5.80; N, 4.20. Mass spectrum (CI): m/z: 659 ([MH$^+$], 100).

ArN=C(S(CH$_2$)$_2$S)C=NAr (7b, Ar = 2,6-(3,4-(CH$_3$)$_2$C$_6$H$_3$)$_2$-C$_6$H$_3$). Bis(imidoyl) chloride **5b** (2.1 g, 3.0 mmol), 1,2-ethanedithiol (1.43 g, 15.2 mmol), and NaH (364 mg, 15.2 mmol) were used; yellow solid; yield: 0.9 g (42%). ^{1}H NMR (400.13 MHz, C$_2$D$_2$Cl$_4$, 298 K) δ: 7.40 (d, 4H, H$_{\mathrm{arom}}$), 7.26−7.30 (m, 6H, H$_{\mathrm{arom}}$), 7.21 (d, 4H, H$_{\mathrm{arom}}$), 7.03 (d, 4H, H$_{\mathrm{arom}}$), 2.25 (s, 12H, CH$_3$), 2.13 (s, 12H, CH$_3$), 1.99 (s, 4H, CH$_2$). ^{13}C NMR (100.16 MHz, C$_2$D$_2$Cl$_4$, 298 K) δ: 153.87, 145.00, 136.73, 135.59, 134.83, 131.12, 131.04, 129.07, 128.97, 127.10, 124.85, 30.20, 19.60, 19.56. Anal. Calcd for C$_{48}$H$_{46}$N$_2$S$_2$: C, 80.63; H, 6.48; N, 3.92. Found: C, 80.49; H, 6.43; N, 3.88. Mass spectrum (CI): m/z: 715 ([MH$^+$], 100).

General Procedure for Synthesis of the Nickel(II) Complexes. A procedure reported previously was used to synthesize the nickel(II) complexes.[4,14] In a 100 mL Schlenk flask, the diimine (1 equiv) and Ni(acac)$_2$ (1 equiv) were placed and dissolved in methylene chloride (50 mL). [CPh$_3$][B(C$_6$F$_5$)$_4$] (1 equiv) in methylene choride (15 mL) was added slowly using a syringe. The resultant dark-red solution was stirred overnight. The solution was filtered through an alumina column, using methylene chloride as eluent. The volume was reduced to 15 mL and *n*-pentane was added slowly to precipitate the complex. The slightly colored supernatant was decanted and the precipitate was dissolved in methylene chloride (15 mL). The procedure was repeated four times. The pure product was dried in vacuo to yield a red powder.

[(ArN=C(CH$_3$)−C(CH$_3$)=NAr)Ni(acac)]B(C$_6$F$_5$)$_4$ (8a, Ar = 2,6-(3-(CH$_3$)C$_6$H$_4$)$_2$C$_6$H$_3$). Diimine **6a** (1.34 g, 2.24 mmol), Ni(acac)$_2$ (577 mg, 2.24 mmol), and [CPh$_3$][B(C$_6$F$_5$)$_4$] (2.1 g, 2.28 mmol) were used; red solid, yield: 2.7 g (84%). ^{1}H NMR (400.13 MHz, C$_2$D$_2$Cl$_4$, 298 K) δ: 7.50 (t, 2H, H$_{\mathrm{arom}}$), 7.28−7.32 (m, 12H, H$_{\mathrm{arom}}$), 7.09 (s, 4H, H$_{\mathrm{arom}}$), 7.02 (d, 4H, H$_{\mathrm{arom}}$), 5.41 (s, 1H, CH), 2.37 (s, 12H, CH$_3$), 1.61 (s, 6H, CH$_3$), 1.43 (s, 6H, CH$_3$). Anal. Calcd for C$_{73}$H$_{47}$BF$_{20}$N$_2$NiO$_2$: C, 61.16; H, 3.30; N, 1.95. Found: C, 61.29; H, 3.35; N, 1.85. Mass spectrum (MALDI): m/z: 753.1 ([M$^+$ − borate], 100).

[(ArN=C(CH$_3$)−-C(CH$_3$)=NAr)Ni(acac)]B(C$_6$F$_5$)$_4$ (8b, Ar = 2,6-(3,4-(CH$_3$)$_2$C$_6$H$_3$)$_2$C$_6$H$_3$). Diimine **6b** (1.0 g, 1.53 mmol), Ni(acac)$_2$ (394 mg, 1.53 mmol), and [CPh$_3$][B(C$_6$F$_5$)$_4$] (1.41 g, 1.53 mmol) were used; red solid; yield: 1.95 g (85%). ^{1}H NMR (400.13 MHz, C$_2$D$_2$Cl$_4$, 298 K) δ: 7.50 (t, 2H, H$_{\mathrm{arom}}$), 7.31 (d, 4H, H$_{\mathrm{arom}}$), 7.15 (d, 4H, H$_{\mathrm{arom}}$), 7.11 (s, 4 H, H$_{\mathrm{arom}}$), 7.06 (d, 4 H, H$_{\mathrm{arom}}$), 5.30 (s, 1H, CH), 2.36 (s, 12H, H$_{\mathrm{arom}}$), 2.27 (s, 12H, CH$_3$), 1.55 (s, 6H, CH$_3$), 1.40 (s, 6H, CH$_3$). Anal. Calcd for C$_{77}$H$_{55}$BF$_{20}$N$_2$NiO$_2$: C, 62.08; H, 3.72; N, 1.88. Found: C, 62.03; H, 3.78; N, 1.86. Mass spectrum (MALDI): m/z: 809.5 ([M$^+$ − borate], 100).

[(ArN=C(CH$_3$)−C(CH$_3$)=NAr)Ni(acac)]B(C$_6$F$_5$)$_4$ (8c, Ar = 2,5-(3,5-(CH$_3$)$_2$C$_6$H$_3$)$_2$C$_6$H$_3$). Diimine **6c** (1.3 g, 1.99 mmol), Ni(acac)$_2$ (512 mg, 1.99 mmol), and [CPh$_3$][B(C$_6$F$_5$)$_4$] (1.84 g, 1.99 mmol) were used; red solid; yield: 2.5 g (84%). ^{1}H NMR (400.13 MHz, C$_2$D$_2$Cl$_4$, 298 K) δ: 7.78 (d, 2H, H$_{\mathrm{arom}}$), 7.66 (s, 4H, H$_{\mathrm{arom}}$), 7.54 (d, 2H, H$_{\mathrm{arom}}$), 7.25 (s, 4H, H$_{\mathrm{arom}}$), 7.18 (s, 2H, H$_{\mathrm{arom}}$), 7.14 (s, 4H, H$_{\mathrm{arom}}$), 5.50 (s, 1H, CH), 2.53 (s, 12H, CH$_3$), 2.46 (s, 12H, CH_3), 1.75 (s, 6H, CH_3), 1.65 (s, 6H, CH_3). Anal. Calcd for $C_{77}H_{55}BF_{20}N_2NiO_2$: C, 62.08; H, 3.72; N, 1.88. Found: C, 61.94; H, 3.68; N, 1.86. Mass spectrum (MALDI): *m*/*z*: 809.5 ([M^+ − borate], 100).

[(ArN=C(CH$_3$)−C(CH$_3$)=NAr)Ni(acac)]B(C$_6$F$_5$)$_4$ (8d, Ar = 2,5-(4-(C(CH$_3$)$_3$)C$_6$H$_4$)$_2$C$_6$H$_3$). Diimine **6d** (1.2 g, 1.57 mmol), $Ni(acac)_2$ (403 mg, 1.57 mmol), and $[CPh_3][B(C_6F_5)_4]$ (1.45 g, 1.57 mmol) were used; red solid; yield: 1.95 g (78%). There are existing two isomers. Isomer 1: 64%. Isomer 2: 36%. ^1H NMR (400.13 MHz, $C_2D_2Cl_4$, 298 K) δ: 7.71−7.77 (m, 10H, H_{arom}), 7.54−7.60 (m, 12 H, H_{arom}), 5.43 (s, 1H, CH, isomer 1), 5.36 (s, 1H, CH, isomer 2), 1.95 (s, 6H, CH_3, isomer 1), 1.81 (s, 6H, CH_3, isomer 2), 1.59 (s, 6H, CH_3, isomer 1), 1.55 (s, 6H, CH_3, isomer 2), 1.37−1.41 (m, 36H, CH_3). Anal. Calcd for $C_{85}H_{71}BF_{20}N_2NiO_2$: C, 63.73; H, 4.47; N, 1.75. Found: C, 63.61; H, 4.51; N, 1.72. Mass spectrum (MALDI): *m*/*z*: 921.6 ([M^+ − borate], 100).

[(ArN=C(S(CH$_2$)$_2$S)C=NAr)Ni(acac)]B(C$_6$F$_5$)$_4$ (9a, Ar = 2,6-(3-(CH$_3$)C$_6$H$_4$)$_2$C$_6$H$_3$). Dithiane-bridged diimine **7a** (1.1 g, 1.67 mmol), $Ni(acac)_2$ (429 mg, 1.67 mmol), and $[CPh_3]$-$[B(C_6F_5)_4]$ (1.54 g, 1.67 mmol) were used; red solid; yield: 2.3 g (92%). ^1H NMR (400.13 MHz, $C_2D_2Cl_4$, 298 K) δ: 7.51 (t, 2H, H_{arom}), 7.30−7.33 (m, 12H, H_{arom}), 7.20−7.24 (m, 8H, H_{arom}), 5.32 (s, 1H, CH), 2.65 (s, 4H, CH_2), 2.37 (s, 12H, CH_3), 1.58 (s, 6H, CH_3). Anal. Calcd for $C_{73}H_{45}BF_{20}N_2NiO_2S_2$: C, 58.62; H, 3.03; N, 1.87. Found: C, 58.49; H, 3.05; N, 1.81. Mass spectrum (MALDI): *m*/*z*: 815.3 ([M^+ − borate], 100).

[(ArN=C(S(CH$_2$)$_2$S)C=NAr)Ni(acac)]B(C$_6$F$_5$)$_4$ (9b, Ar = 2,6-(3,4-(CH$_3$)$_2$C$_6$H$_3$)$_2$C$_6$H$_3$). Dithiane-bridged diimine **7b** (1.2 g, 1.68 mmol), $Ni(acac)_2$ (431 mg, 1.68 mmol), and $[CPh_3][B(C_6F_5)_4]$ (1.55 g, 1.68 mmol) were used; red solid; yield: 2.3 g (88%). ^1H NMR (400.13 MHz, $C_2D_2Cl_4$, 298 K): δ: 7.51 (t, 2H, H_{arom}), 7.32 (d, 4H, H_{arom}), 7.23−7.25 (m, 8H, H_{arom}), 7.13 (d, 4H, H_{arom}), 5.33 (s, 1H, CH), 2.63 (s, 4H, CH_2), 2.36 (s, 12H, CH_3), 2.28 (s, 12H, CH_3), 1.51 (s, 6H, CH_3). Anal. Calcd for $C_{77}H_{53}BF_{20}N_2NiO_2S_2$: C, 59.59; H, 3.44; N, 1.81. Found: C, 59.65; H, 3.47; N, 1.76. Mass spectrum (MALDI): *m*/*z*: 871.4 ([M^+ − borate], 100).

Synthesis of the Precatalysts. The silica gel SP9−496 was heated at 350 °C in vacuo. The dried silica gel was slurried in dry methylene chloride and the desired amount of the complex was added. The mixture was shaken for 2 h, the solvent was removed in vacuo and the resulting residue was washed two times with dry *n*-pentane and dried in vacuo. For precatalysts **10a1** and **11a1**, the solvent was filtered off and the residue was washed two times with dry *n*-pentane and dried in vacuo.

10a (1 wt % Ni). Silica gel (300 mg), complex **8a** (97 mg), and methylene chloride (5 mL) were used. Theoretical nickel loading: 1 wt %. Anal. Calcd for 1 wt % Ni: C, 14.95. Found: C, 15.95 (1.06 wt % Ni). ICP-AES: 0,973 wt % Ni.

10a1 (0.24 wt % Ni). Silica gel (300 mg), complex **8a** (97 mg), and methylene chloride (5 mL) were used. Theoretical nickel loading: 1 wt %. Anal. Calcd for 1 wt % Ni: C, 14.95. Found: C, 3.61 (0.24 wt % Ni).

10a2 (0.25 wt % Ni). Silica gel (200 mg), complex **8a** (12.9 mg), and methylene chloride (4 mL) were used. Theoretical nickel loading: 0.25 wt %. Anal. Calcd for 0.25 wt % Ni: C, 3.74. Found: C, 3.93 (0.26 wt % Ni).

10b (1 wt % Ni). Silica gel (340 mg), complex **8b** (115.5 mg), and methylene chloride (7 mL) were used. Theoretical nickel loading: 1 wt %. Anal. Calcd for 1 wt % Ni: C, 15.76. Found: C, 16.12 (1.02 wt % Ni).

10c (1 wt % Ni). Silica gel (300 mg), complex **8c** (101.9 mg), and methylene chloride (5 mL) were used. Theoretical nickel loading: 1 wt %. Anal. Calcd for 1 wt % Ni: C, 15.76. Found: C, 15.91 (1.01 wt % Ni).

10d (1 wt % Ni). Silica gel (350 mg), complex **8d** (131.2 mg), and methylene chloride (7 mL) were used. Theoretical nickel loading: 1 wt %. Anal. Calcd for 1 wt % Ni: C, 17.41. Found: C, 17.66 (1.01 wt % Ni).

11a (1 wt % Ni). Silica gel (350 mg), complex **9a** (119.5 mg), and methylene chloride (7 mL) were used. Theoretical nickel loading: 1 wt %. Anal. Calcd for 1 wt % Ni: C, 14.95. Found: C, 14.56 (0,97 wt % Ni).

11a1 (0.27 wt % Ni). Silica gel (320 mg), complex **9a** (109.0 mg), and methylene chloride (7 mL) were used. Theoretical nickel loading: 1 wt %. Anal. Calcd for 1 wt % Ni: C, 14.95. Found: C, 3.98 (0.27 wt % Ni).

11b (1 wt % Ni). Silica gel (300 mg), complex **9b** (107.7 mg), and methylene chloride (7 mL) were used. Theoretical nickel loading: 1 wt %. Anal. Calcd for 1 wt % Ni: C, 15.76. Found: C, 16.19 (1.03 wt % Ni).

General Procedure for Gas Phase Polymerization of Ethylene. Sodium chloride (100 g) was heated at 150 °C. The pressure reactor was evacuated at 110 °C. The dried sodium chloride was put together with the supported catalyst into the reaction vessel. Argon was removed and ethylene (ethylene/hydrogen) was pressured into the reactor and maintained at 5 bar. The reactor was heated up to the desired temperature. The polymerization temperature inside kept constant through an outside water cooling. The polymerization was started by injection TMA (2 M in toluene) through a pressure buret with 10 bar ethylene (ethylene/hydrogen) and was carried out for 1 h at constant pressure. After that time, the reactor was decompressed and the polymer particles were separated by washing in acidified water. The polymer was filtered and dried in vacuo at 80 °C overnight.

General Procedure for Solution Polymerization of Ethylene. The autoclave was evacuated at 125 °C. **9c** (5 μmol) and **9d** (10 μmol) were dissolved in dry methylene chloride (4 mL). Dry toluene (800 mL) was added, followed by the complex solution. Argon was removed and ethylene (ethylene/hydrogen) was pressured into the reactor and maintained at 5 bar. The reactor was heated up to the desired temperature. The polymerization was started by injection TMA (2 M in toluene) through a pressure buret with 10 bar of ethylene (ethylene/hydrogen). The polymerization temperature inside kept constant through an inside water cooling as well as the ethylene pressure. The reaction was carried out for 1 h. After that time, the reactor was decompressed and the reaction mixture was put in acidified methanol and stirred for 1 h. The polymer was filtered and dried in vacuo at 80 °C overnight.

Video Microscopy Experiments. A small metal cylinder with glass plates on the top was placed in a minireactor (200 mL) with a glass window. The reactor was heated at 80 °C in vacuo. A small amount of the precatalyst **10a2** was distributed on the glass plates. TMA (0.1 mL) was placed on the bottom, and the argon atmosphere was exchanged against ethylene (4 bar). The autoclave was heated at 60 °C. Then the camera was started, and images of the particles were recorded.

Acknowledgment. The financial support of E. I. du Pont de Nemours & Co. is gratefully acknowledged.

Note Added after ASAP Publication. This article was published on the web on March 17, 2010. Due to a production error, several values in Table 2 were incorrect. The correct version was published on March 23, 2010.

Supporting Information Available: Crystallographic information file (cif file) for complex **8c**. This material is available free of charge via the Internet at http://pubs.acs.org.

References and Notes

(1) Johnson, L. K.; Killian, C. M.; Brookhart, M. *J. Am. Chem. Soc.* **1995**, *117*, 6414–6415.

(2) (a) Rieger, B.; Baugh, L. S.; Kacker, S.; Striegler, S. *Late Transition Metal Polymerization Catalysis*; Wiley-VCH: Weinheim, Germany, 2003; p 30. (b) Brookhart, M.; Ittel, S. D.; Johnson, L. K. *Chem. Rev.* **2000**, *100*, 1169–1203. (c) Gates, D. P.; Svejda, S. A.; Onate, E.; Killian, C. M.; Johnson, L. K.; White, P. S.; Brookhart, M. *Macromolecules* **2000**, *33*, 2320–2334.

(3) Guan, Z.; Cotts, P. M.; McCord, E. F.; McLain, S. J. *Science* **1999**, *283*, 2059–2062.

(4) Meinhard, D.; Wegner, M.; Kipiani, G.; Hearley, A.; Reuter, P.; Fischer, S.; Othmar, M.; Rieger, B. *J. Am. Chem. Soc.* **2007**, *129*, 9182–9191.
(5) Fink, G.; Steinmetz, B.; Zechlin, J.; Przybyla, C.; Tesche, B. *Chem. Rev.* **2000**, *100*, 1377–1390.
(6) (a) Hlatky, G. G. *Chem. Rev.* **2000**, *100*, 1347–1376. (b) Chien, J. C. W. *Top. Catal.* **1999**, *7*, 23–36.
(7) (a) Mackenzie, P. B.; Moody, L. S.; Killian, C. M.; Lavoie, G. G. (Eastman Chemical Company). Patent PCT WO 99/62968, priority date June 1, **1998**. (b) Simon, L. C.; Patel, H.; Soares, J. B. P.; De Souza, R. F. *Macromol. Chem. Phys.* **2001**, *202*, 3237–3247. (c) Alobaidi, F.; Ye, Z.; Zhu, S. *Macromol. Chem. Phys.* **2003**, *204*, 1653–1659. (d) Dorcier, A.; Merle., N.; Taoufik, M.; Bayard, F.; Lucas, C.; de Mallmann, A.; Basset, J. M. *Organometallics* **2009**, *28*, 2173–2178.
(8) (a) Preishuber-Pflugl, P.; Brookhart, M. *Macromolecules* **2002**, *35*, 6074–6076. (b) Schrekker, H. S.; Kotov, V.; Preishuber-Pflugl, P.; White, P.; Brookhart, M. *Macromolecules* **2006**, *39*, 6341–6354.
(9) Moody, L. S.; Mackenzie, P. B.; Killian, C. M.; Lavoie, G. G.; Ponasik, J. A., Jr.; Barrett, A. G.; Smith, T. W.; Pearson, J. C. (Eastman Chemical Company). Patent PCT WO 00/50470, priority date Feb 22, **1999**.
(10) Tannous, K.; Soares, J. B. P. *Macromol. Chem. Phys.* **2002**, *203*, 1895–1905.
(11) (a) Eberstein, C.; Garmatter, B.; Reichert, K.-H.; Sylvester, G. *Chem. Ing. Tech.* **1996**, *68*, 820–823. (b) Zöllner, K.; Reichert, K.-H. *Chem. Ing. Tech.* **2001**, *73*, 849–852. (c) Zöllner, K.; Reichert, K.-H. *Chem. Eng. Technol.* **2002**, *25*, 707–710.
(12) Pater, J. T. M.; Weickert, G.; Swaaij, W. P. M. *Chimia* **2001**, *55*, 231–233.
(13) Knoke, S.; Ferrari, D.; Tesche, B.; Fink, G. *Angew. Chem., Int. Ed.* **2003**, *42*, 5090–5093.
(14) Schmid, M.; Eberhardt, R.; Klinga, M.; Leskelä, M.; Rieger, B. *Organometallics* **2001**, *20*, 2321–2330.
(15) Böhm, L. L. *Angew. Chem., Int. Ed.* **2003**, *43*, 5010–5030.
(16) (a) Mikenas, T. B.; Zakharov, V. A.; Echevskaya, L. G.; Matsko, M. A. *J. Polym. Sci., Part A: Polym. Chem.* **2005**, *43*, 2128–2133. (b) Semikolenova, N. V.; Zakharov, V. A.; Paukshtis, E. A.; Danilova, I. G. *Top. Catal.* **2005**, *32*, 77–82. (c) Zakharov, V. A.; Semikolenova, N. V.; Mikenas, T. B.; Barabanov, A. A.; Bukatov, G. D.; Echevskaya, L. G.; Matsko, M. A. *Kinet. Catal.* **2006**, *47*, 303–309.
(17) (a) Mikenas, T. B.; Zakharov, V. A.; Echervskaya, L. G.; Matsko, M. A. *J. Polym. Sci., Part A: Polym. Chem.* **2007**, *45*, 5057–5066. (b) Barabanov, A. A.; Bukatov, G. D.; Zakharov, V. A.; Semikolenova, N. V.; Mikenas, T. B.; Echevskaja, L. G.; Matsko, M. A. *Macromol. Chem. Phys.* **2006**, *207*, 1368–1375.
(18) Janiak, C.; Rieger, B. *Angew. Makromol. Chem.* **1994**, *215*, 47–52.
(19) (a) Gibson, V. C. *Science* **2006**, *312*, 703–704. (b) Arriola, D. J.; Carnahan, E. M.; Hustad, P. D.; Kuhlman, R. L.; Wenzel, T. T. *Science* **2006**, *312*, 714–719. (c) Zintl, M.; Rieger, B. *Angew. Chem., Int. Ed.* **2007**, *46*, 333–335.